ISSN 0015-4628, Fluid Dynamics, 2018, Vol. 53, No. 3, pp. 372–384. © Pleiades Publishing, Ltd., 2018.
Original Russian Text © E.I. Mogilevskii, V.Ya. Shkadov, 2018, published in Izvestiya Rossiiskoi Akademii Nauk, Mekhanika Zhidkosti i Gaza, 2018, No. 3, pp. 40–53.

Stability Analysis of a Falling Film Flow Down a Plane with Sinusoidal Corrugations

E. I. Mogilevskii[1]* and V. Ya. Shkadov[1]**

[1] *Lomonosov Moscow State University, Moscow, Russia*

Received December 11, 2017

Abstract—The liquid viscous film falling down a vertical wall with sinusoidal relief is considered. The linear stability of steady-state flow with respect to time-periodic disturbances is studied using the Floquet theory. It is shown that in the case of applying corrugations the variation in the disturbance growth rate is proportional to the second power of their undulations. Depending on the relief parameters there exist two possibilities: the instability domain can expand or certain disturbances can be stabilized. The growth rates are obtained numerically and analytically in the approximation of low-amplitude corrugations. The development of waves from small disturbances is simulated within the framework of nonlinear equations and the formation of structures whose wavelength is significantly greater than the space relief period is found out.

DOI: 10.1134/S0015462818030126

The viscous liquid film flow subject to the gravity force on the surface with a microrelief is actively investigated in connection with many applications [1], being an example of the problem of interaction of the natural hydrodynamic instability with an external periodic impact.

In [2] the system of equations describing nonlinear viscous liquid film flow over a microrelief on an inclined plane was derived. The characteristic streamwise dimension of the corrugations was assumed to be much more than the film thickness and their amplitude be comparable with the latter. The basic idea used in derivation and formulated in [3] consists in the fact that the viscous friction forces ensure the parabolic shape of the streamwise velocity profile in each of the transverse cross-sections. The flow is described by two functions of the streamwise coordinate and time, namely, these are the film thickness h and the local flow rate q, and the equations describe the evolution of these quantities.

In [2] steady-state film flow over a localized and periodic relief was considered. It was shown that the presence of the periodic relied leads to decrease in the fluid flow rate when the mean film thickness is fixed and for the low relief amplitude approximate analytical solutions were obtained. In [4] the more detailed analysis of steady-state flow was given in the framework of the same approach. In [5] other steady-state solutions were found under the assumption that the free-surface period is only multiple to the corrugation period but does not need to coincide with the latter. The solutions obtained exist only for fairly high amplitudes of the relief.

In [6] the problem of stability of steady-state non-Newtonian liquid flow considered in [2, 4] was formulated. This analysis seems to be quite labor-intensive since it contains five dimensionless parameters, namely, the corrugation amplitude and period divided by the film thickness and the characteristic wavelength in the falling film, the slope of the incline, the Reynolds number, and the power in the viscosity law indicating the non-Newtonian properties of the medium. Most attention was concentrated on the dependence of the form of the neutral curve separating the stability and instability domains in the disturbance frequency–Reynolds number plane and the determination of the critical Reynolds number for flow over the inclined plane [4]. It was shown that the film can be stabilized with respect to the low-frequency disturbances for a relatively high corrugation amplitude (up to 40% of the mean film thickness), the instability domain becoming multiply connected and isolated domains called “instability islands” by the authors can develop.

*E-mail: mogilevskiy@mech.math.msu.su.
**E-mail: shkadov@mech.math.msu.su.

The film flow stabilization due to periodic corrugations on the sustaining surface was noted in [7] in which the Newtonian liquid on a vertical surface with sinusoidal corrugations was considered. The corrugation parameters were analyzed for several sets of the flow parameters (the properties of liquid and the flow rate). Surfaces which stabilize flows with respect to any small disturbances were found. All the surfaces corresponded to the corrugation amplitude in tens of percents of the film thickness. The fact that the critical Reynolds number increases in the presence of small corrugations was demonstrated experimentally in [8].

The experiments [9] demonstrated the mechanism of flow stabilization characteristic of the high-amplitude corrugations. If the hollows between the most prominent points on the surface are fairly sharp and deep, they begin to serve as cavities inside which vortices develop. The streamline passing near the rigid surface in the neighborhood of the maximum undulation does not follow it in the hollow but passes above the vortex. Thus, the assumption on the local parabolic profile is not satisfied and the approach developed in [2–7] cannot be applied. In [10] the stability of flow was analyzed within the framework of the linearized Navier–Stokes equations and the results [9] were confirmed by calculations. In [11] the detailed experimental investigation of the linear stability of a film on the inclined plane was outlined.

The effect of the relief on weakly nonlinear waves [12] was considered in [5]. In [13] the solutions of the full Navier–Stokes equations of the type of steady-state waves were obtained. In [14] the development of nonlinear waves was investigated experimentally.

In the present study a particular case of the problem considered in [2, 7] is investigated, namely, falling Newtonian liquid over a vertical wall with sinusoidal corrugations. The stability of flow is investigated in detail for a low corrugation amplitude. The steady-state solution has a fairly simple form and the influence of corrugations can be analytically described. The results of the linear analysis of stability are verified by solving the nonlinear time-dependent equations numerically.

1. FORMULATION OF THE PROBLEM

Let a layer of Newtonian liquid of a density ρ and a viscosity $\mu = \nu\rho$ flow down along the vertical plane with a periodic sinusoidal relief subject to the gravity force. The Ox^* axis of the Cartesian coordinate system is directed downwards and located so that the mean surface deviation from the axis is equal to zero, the Oy^* axis is horizontal and directed towards the liquid, and the Oz^* axis supplements the reference frame to the right-handed coordinate system. The rigid surface is described by the equation $y^* = h_0^*(x^*)$ and the free surface on which the surface tension with a coefficient σ acts is described by the equation $y^* = h_1^*(t^*, x^*)$, where t^* is time. The asterisk denotes the dimensional quantities.

Let the thickness of the film falling down the smooth plane with a given flow rate be the scale of the transverse coordinate while the scale of the streamwise coordinate be greater by ε^{-1} times (quantity $\varepsilon \ll 1$ will be defined below). Assuming that in each of the cross-sections the streamwise velocity profile represents a parabola, integration of the Navier–Stokes equations across the layer leads to the following system of equations if the terms of the order of ε^2 and $\varepsilon\mathrm{Re}^{-1}$ are assumed to be small (detailed derivation is given in [2])

$$h_t + q_x = 0,$$
$$q_t + \frac{6}{5}\left(\frac{q^2}{h}\right)_x = \frac{1}{5\delta}\left(hh_{xxx} - \frac{q}{h^2} + h\right) + \frac{h}{5\delta}h_{0xxx}. \tag{1.1}$$

Here, $h(t,x) = h_1(t,x) - h_0(x)$ is the film thickness and q is the local flow rate. The dimensionless parameter δ can be determined from the condition [15] which means that the viscous, gravitational, and capillary forces are of the same order

$$\frac{\varepsilon^2}{\mathrm{We}} = \frac{3}{\varepsilon\mathrm{Re}} = \frac{1}{5\delta}, \quad \mathrm{We} = \frac{\rho U^2 H}{\sigma}, \quad \mathrm{Re} = \frac{UH}{\nu}. \tag{1.2}$$

The characteristic velocity U and the film thickness H are connected by the relations following from the fact that the flow rate is fixed $UH = Q^*$ and the steady-state flow on the plane wall is described by the Nusselt solution: $U = gH^2/(3\nu)$ (g is the gravity acceleration). The parameter ε can be determined from the relation $\varepsilon^2/\mathrm{We} = 3/(\varepsilon\mathrm{Re})$ which follows from (1.2). At large values of the Kapitsa number $\gamma = \sigma\left(\rho^3 g\nu^4\right)^{-1/3}$ (for water at room temperature $\gamma \approx 3300$) the conditions ε^2 and $\varepsilon\mathrm{Re}^{-1} \ll 1$ adopted

in deriving (1.1) are fulfilled. A generalization of Eqs. (1.1) to include the case of small values of γ by taking into account the terms of the order of ε^2 is given in [16].

Let $h_0(x) = a\cos\alpha x$. When $a \ll 1$ the approximate steady-state solution of (1.1) takes the form $h_s = 1 + h^{(0)} + h^{(1)}e^{i\alpha x} + \overline{h^{(1)}}e^{-i\alpha x}$ [2] (bar denotes complex conjugate):

$$h^{(1)} = \frac{i}{2}\frac{\alpha^3}{3 - i\alpha(\alpha^2 - 6\delta)}a + O(a^3), \quad h^{(0)} = 4|h^{(1)}|^2 + O(a^4). \tag{1.3}$$

In the case of finite corrugation amplitude the shape of the free surface can be determined as the result of numerical solution of a system of algebraic equations with respect to the expansion coefficients of the unknown function in the Fourier series

$$h_s = 1 + \sum_{k=-N}^{N} h^{(k)}\exp(ik\alpha x), \quad h^{(-k)} = \overline{h^{(k)}}.$$

As $a \to 0$, the terms $h^{(\pm k)}\exp(\pm ik\alpha x), k \neq 0$ have the order $O(a^k)$ and $h^{(0)} = O(a^2)$.

When $\delta = 0.2$ and $a = 0.2$ the numerical solution differs from the approximate analytical solution (1.3) by no more than 4% for all α. A detailed analysis of the steady-state solution is given in [4].

In what follows, we will consider both the spatial development of small disturbances of the steady-state solution and the time-periodic solutions of (1.1).

2. LINEAR STABILITY ANALYSIS

Let

$$h(t,x) = h_s(x) + h_d(t,x), \quad q(t,x) = 1 + q_d(t,x), \quad h_d, q_d \ll 1.$$

Linearization of (1.1) gives the following equations with respect to small disturbances (subscript d is omitted)

$$h_t + q_x = 0,$$
$$q_t + \frac{6}{5}\left[2\frac{q_x}{h_s} - \frac{h_x}{h_s^2}h_x - 2\frac{h_s'}{h_s^2}q + 2\frac{h_s'}{h_s^3}h_x\right] = \frac{1}{5\delta}\left[h\left(\frac{6\delta}{h_s}\left(\frac{1}{h_s}\right)' + \frac{3}{h_s^3}\right) + h_{xxx}h_s - \frac{q}{h_s^2}\right]. \tag{2.1}$$

The coefficients of this equation depend only on x; therefore, in order to determine the stability of flow it is sufficient to consider the spatial development of time-periodic disturbances. Let

$$q = Q_1(x)e^{-i\omega t}, \quad h = H_1 e^{-i\omega t}, \quad \omega = \text{const}. \tag{2.2}$$

For Q_1 we obtain the following ordinary differential equation with periodic coefficients (subscript 1 is omitted):

$$Q^{\mathrm{IV}} = -\frac{6\delta}{h_s^3}Q'' + \frac{1}{h_s^4}\left[18\delta h_s' - 3 + i12\delta\omega h_s^2\right]Q' + \frac{1}{h_s^3}\left[5\delta\omega^2 h_s^2 + i\omega\left(1 - 12\delta h_s'\right)\right]Q. \tag{2.3}$$

In [4, 7] similar equations were obtained; however, the parameter δ was not used and the spatial corrugation period was taken as the length scale. This complicates comparison of the results of the film stability analysis on the sinusoidal and plane walls.

In what follows, we will give the main results of solving the problem of stability of the film falling down the vertical wall. Such a solution is unstable to longwave disturbances at any Reynolds numbers [3, 15]. Under the assumption of long waves [17] the solution of the Orr–Sommerfeld equation gives the expression $\beta_n = \sqrt{18\delta}$ for the wavenumber β of neutral disturbances. Linearization of Eqs. (2.1) for integral characteristics leads to the similar expression $\beta_n = \sqrt{15\delta}$. Both methods predict the same phase velocity of neutral disturbances $c_n = 3$. Despite of the difference in the coefficients, the equations for integral characteristics adequately reproduce the form of the neutral curve and fairly exactly predict the nonlinear wave parameters [18]. In [19] it was shown that outside a small vicinity of the corner point on the neutral curve, in which the waves are not of practical interest as a result of small amplitudes, small growth rates, and considerable instability, the neutral curves [3] agree in the most extent with the

Roots of the characteristic equations and parameters of time-periodic disturbances

β	ω	c	I
$0.618 - 0.117i$	1.5	2.42	0.117
$0.312 + 1.44i$	1.5	4.81	-1.44
$-1.99 - 0.336i$	1.5	-0.754	0.336
$1.06 - 0.985i$	1.5	1.42	0.985
0.618	$1.483 + 0.250i$	2.40	0.104
0.618	$-0.19 \times 10^{-4} - 1.25i$	-0.30×10^{-4}	4.06×10^4

corresponding curves of the exact Orr–Sommerfeld equation for the film on the vertical and inclined surfaces.

The coefficients of Eq. (2.3) are constant when there are no corrugations. The solution has the form $Q(x) = Q_0 \exp(i\beta x)$, where β must satisfy the characteristic equation

$$-\beta^4 + 6\delta\beta^2 - (12\delta\omega + 3i)\,\beta + \left(5\delta\omega^2 + i\omega\right) = 0. \tag{2.4}$$

The same equation describes disturbances with a fixed real wavenumber β and unknown parameter ω. Relation (2.4) represents the forth-order equation with respect to β at a fixed ω or the quadratic equation with respect to ω at a fixed β. The first approach simulates the spatial development of deviations from the equilibrium state introduced periodically in time in a certain cross-section, while the second describes the evolution of space-periodic disturbances introduced into the system at the initial instant. The real pairs (β, ω) which satisfy Eq. (2.4) correspond to the neutral disturbances. The phase velocity and the growth rate of the disturbances are connected with the solutions of Eq. (2.4) by the relations $c = \omega/\beta_r$, $c = \omega_r/\beta$ and $I = -\beta_i$, $I = \omega_i\beta/\omega_r$ for the two approaches, respectively; the subscripts r and i denote the real and imaginary parts. In Table 1 we have reproduced the values of the roots of Eq. (2.4), the phase velocities, and the growth rates for $\delta = 0.2$ and $\omega = 1.5$ ($\beta = 0.618$).

Within the framework of each approach, one of the branches of the solutions ω_1 and β_1 describes the waves with the phase velocity close to 3 and a small absolute value of the growth rate. On this branch the roots of Eq. (2.4) are close to the eigennumbers of the spectral problem for the Orr–Sommerfeld equation with the maximum growth rate. In describing the space-periodic solutions, the second branch ω_2 corresponds to disturbances attenuated with time and can have any sign depending on the parameters. Thus, the equations (2.1) adequately describe the time evolution of space-periodic disturbances.

In addition to the root considered above, the equation (2.4) considered as an equation for β has still three roots. In this case β_2 has a positive phase velocity and a negative growth rate, i.e., describes the damped disturbances, β_3 has a negative phase velocity and a positive growth rate, and β_4 has a positive phase velocity and a large positive growth rate. Formally, the presence of the root β_4 implies the definite conclusion on the instability of flow. This contradicts to the experiments.

In order to resolve this contradiction we will investigate the boundary-value problem for Eq. (2.1) on a fairly long interval $x \in [0, L]$. Let Q and Q' be specified in the inlet cross-section $x = 0$ in the form (2.2). This is equivalent to specifying the perturbations of the flow rate and the shape of the free surface. In [21, 22], in considering nonlinear waves on a finite spatial interval, the following non-reflecting boundary conditions are imposed in the outlet cross-section

$$\frac{\partial q}{\partial t} = c\frac{\partial q}{\partial x}, \quad \frac{\partial h}{\partial t} = c\frac{\partial h}{\partial x},$$

where c is a certain positive constant. This can be reduced to the conditions with respect to Q

$$-i\omega Q = cQ', \quad -i\omega Q' = cQ''.$$

The coefficients C_3 and C_4 of the expansions of the solution of the above boundary-value problem in terms of the linearly independent solutions $Q = C_1 \exp(i\beta_1 x) + C_2 \exp(i\beta_2 x) + C_3 \exp(i\beta_3 x) + C_4 \exp(i\beta_4 x)$ tend to zero as $L \to \infty$ for all positive c. If c varies from 1 to 5 for a fixed fairly large L,

then the constants C_1 and C_2 will vary within the limits of 10^{-3}, C_3 is of the order of 10^{-3}, and C_4 is of the order of 10^{-40}. The calculations were carried out at $L = 50$. Thus, in analyzing the stability of flow, it is necessary to ignore the root of the characteristic equation with the negative imaginary part of large absolute value and investigate the influence of corrugations on the roots β_1 and β_2.

If the rigid surface has corrugations then the function $h_s(x)$ differs from unity and the coefficients (2.3) are periodic functions of x. In order to study the stability of the steady-state solution it is necessary to find the Floquet multipliers μ_k, i.e., the eigenvalues of the operator which places the vector of the initial conditions $(Q(0), Q'(0), Q''(0), Q'''(0))^T$ in correspondence with the vector $(Q(2\pi/\alpha), Q'(2\pi/\alpha), Q''(2\pi/\alpha), Q'''(2\pi/\alpha))^T$.

The Floquet multipliers are the eigenvalues of the monodromy matrix. Its components can be found numerically by means of fourfold integration of Eq. (2.3) with various linearly independent initial conditions. The growth rate is determined by the formula [20]

$$I = \ln|\mu_k|\frac{\alpha}{2\pi}.$$

The flow is unstable if the multiplier for which the growth rate tends to $-\beta_{1i}$, as the corrugation amplitude tends to zero, lies outside the unit circle in the complex plane.

The value of the growth rate can be obtained approximately if $a \ll 1$. The steady-state solution takes the form:

$$h_s(x) = 1 + a\left(H^{(1)}e^{i\alpha x} + \overline{H^{(1)}}e^{-i\alpha x}\right) + a^2(H^{(0)} + H^{(2)}e^{i2\alpha x} + \overline{H^{(2)}}e^{-i2\alpha x}) + O(a^3),$$

$$H^{(1)} = \frac{i}{2}\frac{\alpha^3}{3 - i\alpha(\alpha^2 - 6\delta)}, \quad H^{(0)} = 4H^{(1)}\overline{H^{(1)}}.$$

The expression for $H^{(2)}$ can be obtained from (1.1); however, it is not significant for the further considerations.

Equation (2.3) can be expanded in powers of a

$$LQ = \left(L_0 + aL_1 + a^2L_2\right)Q = 0, \tag{2.5}$$

where

$$L_0 = \frac{d^4}{dx^4} + 6\delta\frac{d^2}{dx^2} + (3 - 12i\delta\omega)\frac{d}{dx} - (5\delta\omega^2 + i\omega),$$

$$L_1 = L_1^+ + L_1^-,$$

$$L_2 = L_2^0 + L_2^+ + L_2^-,$$

$$L_1^+ = \left(A_2^1\frac{d^2}{dx^2} + A_1^1\frac{d}{dx} + A_0^1\right)\exp^{i\alpha x}, \quad L_1^- = \left(B_2^1\frac{d^2}{dx^2} + B_1^1\frac{d}{dx} + B_0^1\right)\exp^{-i\alpha x},$$

$$L_2^0 = \left(D_2\frac{d^2}{dx^2} + D_1\frac{d}{dx} + D_0\right), \quad L_2^+\left(A_2^2\frac{d^2}{dx^2} + A_1^2\frac{d}{dx} + A_0^2\right)\exp^{i2\alpha x},$$

$$L_2^- = \left(B_2^2\frac{d^2}{dx^2} + B_1^2\frac{d}{dx} + B_0^2\right)\exp^{-i2\alpha x},$$

$$A_2^1 = -18\delta H^{(1)}, \quad B_2^1 = -18\delta\overline{H^{(1)}},$$

$$A_1^1 = (-12 + 24i\omega\delta - 18i\delta\alpha)H^{(1)}, \quad B_1^1 = (-12 + 24i\omega\delta + 18i\delta\alpha)\overline{H^{(1)}},$$

$$A_0^1 = (5\delta\omega^2 - 12\omega\delta\alpha + 3i\omega)H^{(1)}, \quad B_0^1 = (5\delta\omega^2 + 12\omega\delta\alpha + 3i\omega)\overline{H^{(1)}},$$

$$D_2 = 0, \quad D_1 = (12 + 24i\delta\omega)H^{(1)}\overline{H^{(1)}}, \quad D_0 = 10\delta\omega^2H^{(1)}\overline{H^{(1)}}.$$

The expressions for A_n^2 and B_n^2 are not significant. Let the general solution of (2.5) have the form $Q = Q_0 + aQ_1 + a^2Q_2$. Substitution of such a solution in the equation with equating the multipliers of the powers of a to zero gives

$$L_0Q_0 = 0,$$

$$L_0Q_1 = -L_1Q_0,$$
$$L_0Q_2 = -L_1Q_1 - L_2Q_0. \tag{2.6}$$

The general solution of the first equation is as follows:

$$Q_0 = \sum_{j=1}^{4} C_j e^{i\beta_j x},$$

where β_j are the roots of the characteristic equation (2.4).

The second equation is inhomogeneous and there is an exponential polynomial with the exponents $i(\beta \pm \alpha)$ on its right-hand side. Since α is a real number and there is no pair with coinciding imaginary part among the roots of (2.4), there is no resonance; consequently, the general solution of the second equation has the form:

$$Q_1 = Q_1^0 + Q_1^+ + Q_1^-,$$
$$Q_1^0 = \sum_{j=1}^{4} C_j^1 e^{i\beta_j x}, \quad Q_1^+ = C_j^{1+} e^{i(\beta_j+\alpha)}, \quad Q_1^- = C_j^{1-} e^{i(\beta_j-\alpha)}.$$

All the terms of the form $C_j e^{i\beta_j x}$ are contained only in Q_0 so that $C_j^1 = 0$ and

$$C_j^{1\pm} = -C_j \frac{L_1^{\pm} e^{i\beta_j}}{L_0 e^{i(\beta_j \pm \alpha)}}.$$

If only one of the constants C_j is nonzero, then for all x

$$Q_0(x + 2\pi/\alpha) + aQ_1(x + 2\pi/\alpha) = (Q_0(x) + aQ_1(x)) \exp\left(i\frac{2\pi\beta_j}{\alpha}\right),$$

consequently, the growth rates do not change in the first approximation in a.

On the right-hand side of the third of equations (2.6) there are terms with the exponents $i\beta_j \pm 2\alpha$, namely, $-\left(L_2^{\pm}Q_0 + L_1^{\pm}Q_1^{\pm}\right)$, and with the exponents $i\beta_j$ which have the form $-\left(L_2^0 Q_0 + L_1^{\pm}Q_1^{\mp}\right)$. The second group of the terms leads to resonance and the particular solution has the form:

$$Q_2 = \sum_{j=1}^{4} C_j^{20} x e^{i\beta_j x} + C_j^{2+} e^{i(\beta_j+2\alpha)x} + C_j^{2+} e^{i(\beta_j-2\alpha)x},$$
$$C_j^{20} = -C_j \left[L_0\left(x e^{i\beta_j x}\right)\right]^{-1} \left[L_2^0 e^{i\beta_j x} - \frac{L_1^{\mp} e^{i\beta_j x}}{L_0 e^{i(\beta_j \mp \alpha)x}} L_1^{\pm} e^{i(\beta_j \mp \alpha)x}\right].$$

The expressions for $C_j^{2\pm}$ are not significant. Let only a single constant C_j be nonzero. Then we have

$$\begin{pmatrix} Q(\frac{2\pi}{\alpha}) \\ Q'(\frac{2\pi}{\alpha}) \\ Q''(\frac{2\pi}{\alpha}) \\ Q'''(\frac{2\pi}{\alpha}) \end{pmatrix} = \begin{pmatrix} Q(0) \\ Q'(0) \\ Q''(0) \\ Q'''(0) \end{pmatrix} \exp\left(i\frac{2\pi\beta_j}{\alpha}\right) + a^2 C_j^{20} \frac{2\pi}{\alpha} \begin{pmatrix} 1 \\ i\beta_j \\ -\beta_j^2 \\ -i\beta_j^3 \end{pmatrix} \exp\left(i\frac{2\pi\beta_j}{\alpha}\right)$$
$$= \begin{pmatrix} Q(0) \\ Q'(0) \\ Q''(0) \\ Q'''(0) \end{pmatrix} \exp\left(i\frac{2\pi\beta_j}{\alpha}\right) + a^2 \frac{C_j^{20}}{C_j} \frac{2\pi}{\alpha} \begin{pmatrix} Q_0(0) \\ Q_0'(0) \\ Q_0''(0) \\ Q_0'''(0) \end{pmatrix} \exp\left(i\frac{2\pi\beta_j}{\alpha}\right)$$

$$= \begin{pmatrix} Q(0) \\ Q'(0) \\ Q''(0) \\ Q'''(0) \end{pmatrix} \left(1 + a^2 \frac{C_j^{20}}{C_j} \frac{2\pi}{\alpha}\right) \exp\left(i \frac{2\pi\beta_j}{\alpha}\right) + O(a^3).$$

Thus, correct to the small terms of the third order, the Floquet multiplier takes the form:

$$\mu_j = \left(1 + a^2 \frac{C_j^{20}}{C_j} \frac{2\pi}{\alpha}\right) e^{i\frac{2\pi\beta_j}{\alpha}}$$

and the growth rate is

$$I = -\beta_{ji} + a^2 \left(\frac{C_j^{20}}{C_j}\right)_r + O(a^3).$$

In Fig. 1 we have reproduced the graphs of the growth rate as a function of the relief wavenumber at a fixed frequency of the inserted disturbances $\omega = 1.5$ and $\omega = 4.5$ for $\delta = 0.2$. In the calculations the relief amplitude $a = 0.2$. Both frequencies correspond to unstable disturbances on the flat wall with the growth rates $I = 0.116$ and $I = 0.01$ respectively; the first quantity is close to the maximum possible growth rate and the neutral disturbances have the frequency $\omega_n = 3\sqrt{3}$. The relief wavenumber is divided by $\sqrt{15\delta}$ which corresponds to the wavenumber of the neutral disturbances on the flat wall. The growth rate decreases sharply at some relief wavenumber and the absolute value of this change depends only slightly on the disturbance frequency; therefore, the disturbances that have a small growth rate on the flat wall are stabilized.

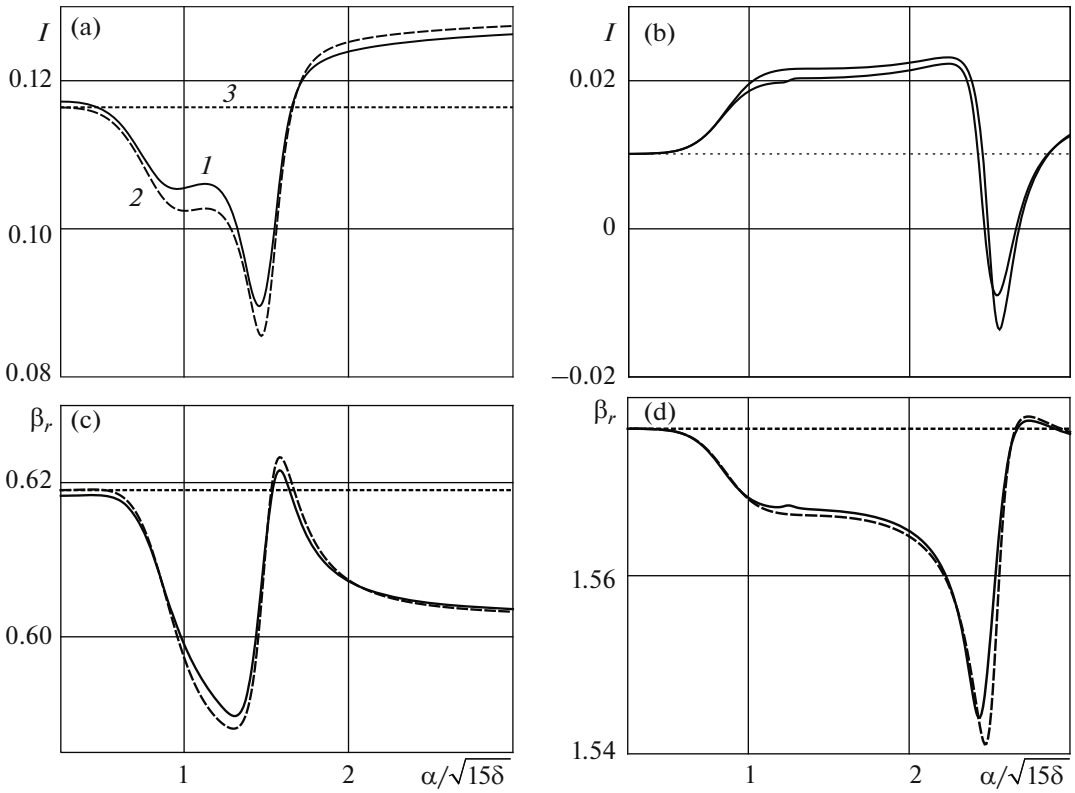

Fig. 1. Disturbance growth rates (a, b) and wavenumbers (c, d) as functions of the normalized relief wavenumber. Curve *1* corresponds to the numerical solution, curve *2* to the approximate analytical solution, and curve *3* to the solution for the flat wall; a and c correspond to $\omega = 1.5$ and b and d to $\omega = 4.5$.

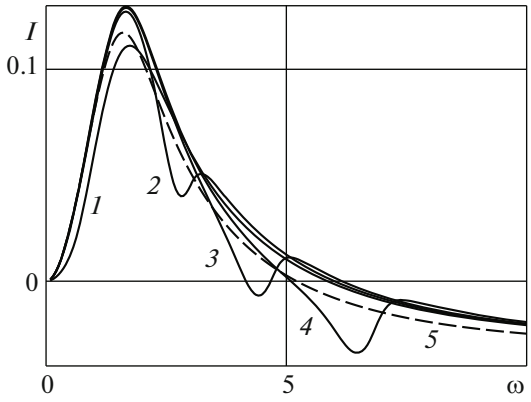

Fig. 2. Disturbance growth rate as a function of the frequency: curves *1–4* correspond to $s = 1$, 2, 2.5, and 3, respectively, and curve *5* to the solution for the flat wall.

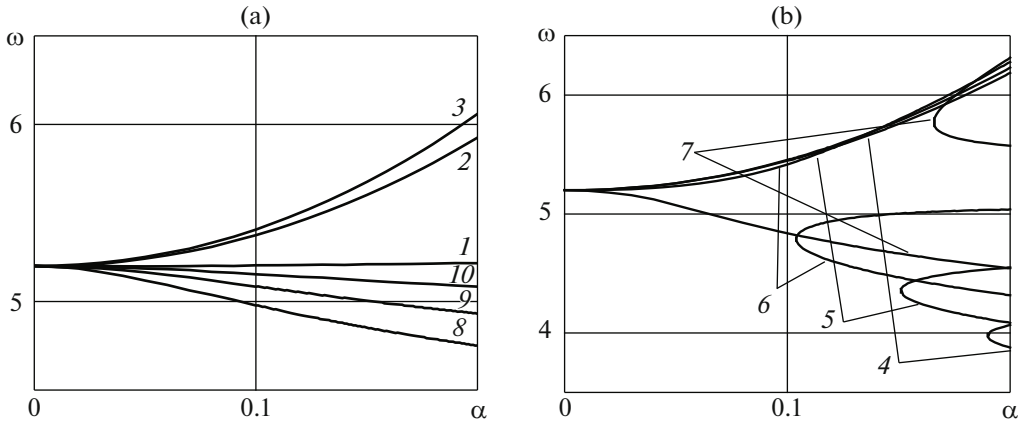

Fig. 3. Neutral curves for various relief wavenumbers: curves *1–10* correspond to $s = 0.5$, 1, 1.5, 2.4, 2.5, 2.6, 2.7, 2.8, 2.9, and 3, respectively.

In Fig. 2 we have reproduced the graphes of the growth rate as a function of the the disturbance frequency at a fixed amplitude for various relief wavenumbers. If the normalized relief wavenumber $s = \alpha/\sqrt{15\delta}$ is small then the relative deviation of the wavenumber of the appearing disturbances on the wall with corrugations from the value on the flat wall is not greater than 10^{-2}. Starting from a certain s, which is close to 1, a frequency range appears such that for these frequencies the growth rate is smaller than that on the flat wall. The resonance frequency at which the relief effect is strongest increases with the wavenumber. This is appreciably manifested if $s > 1$, i.e., the waves, which have the same period as the relief, damp on the flat wall. At the fixed disturbance frequency the relative perturbation of the wavenumber is small.

Since the stabilization is possible at certain frequencies due to the interaction between the disturbances and the relief, the neutral curve has several components of connectivity in the plane (a, ω). For small and large s the neutral frequency is almost independent of the corrugation amplitude.

If s is close to unity, the instability domain extends (curves *1–3* in Fig. 3,a). If the relief effect is manifested in the strongest way for the disturbances with small growth rates and these disturbances are stabilized, the second branch of the neutral curve appears in the plane (a, ω) over the high-amplitude range (Fig. 3,b). As the corrugation wavenumber increases, the second branch displaces towards increase in the frequencies and decrease in the amplitudes. After its intersection with the first branch, the form of the instability domain changes: one branch of the neutral curve goes from the point corresponding to the flat wall towards decrease in the frequency with increase in the amplitude, an instability domain being present over the range of large amplitudes and high frequencies. As s increases, the second instability domain leaves the amplitude range considered and again only a single branch of

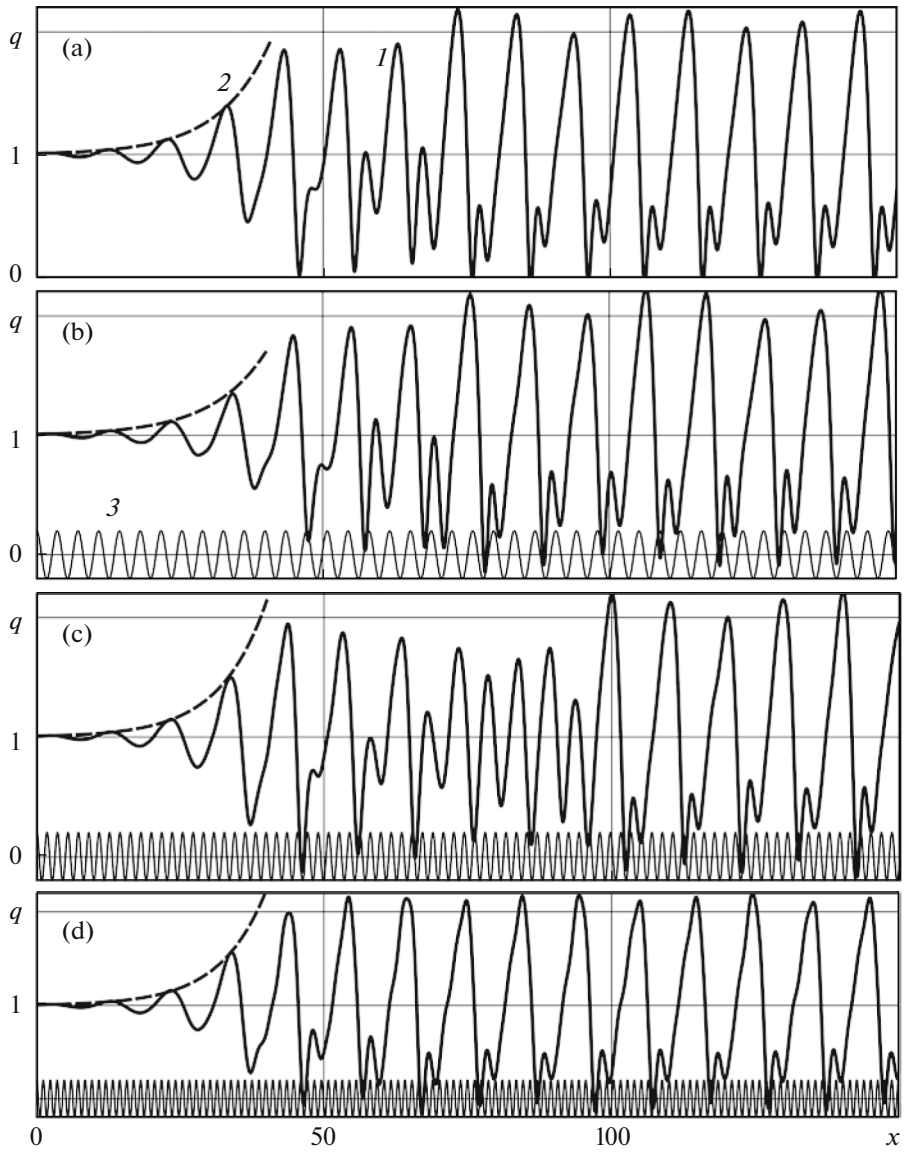

Fig. 4. Profiles of the low-frequency nonlinear waves: a corresponds to $a = 0$ and b–d to $s = 1, 2$, and 3, respectively; curves *1* correspond to the free surface, curves *2* to the result of the linear stability theory, and curves *3* to the rigid surface.

the neutral curve remains. This branch tends to the line $\omega = 3\sqrt{15\delta}$. This corresponds to the flat wall (curves *8–10* in Fig. 3,a).

3. NONLINEAR WAVES

Let the film thickness $h(t)$ and the flow rate $q(t)$ be specified as periodic functions of time in the cross-section $x = 0$. Since, generally speaking, these functions do not satisfy the boundary conditions for the steady-state solution of (1.1), this means that some disturbances are introduced into the system at a certain frequency. From the physical considerations it makes sense to search a solution bounded as $x \to \infty$. The boundary conditions of this type cannot be implemented in the calculations; therefore, we will solve the problem on a finite, although fairly long, interval $x \in [0; L]$ and will set "soft" boundary conditions on the right boundary. These boundary conditions will not reflect the waves arriving at the boundary. Following [21, 22], we will set them in the form:

$$\frac{\partial q}{\partial t} = c\frac{\partial q}{\partial x}, \quad \frac{\partial h}{\partial t} = c\frac{\partial h}{\partial x},$$

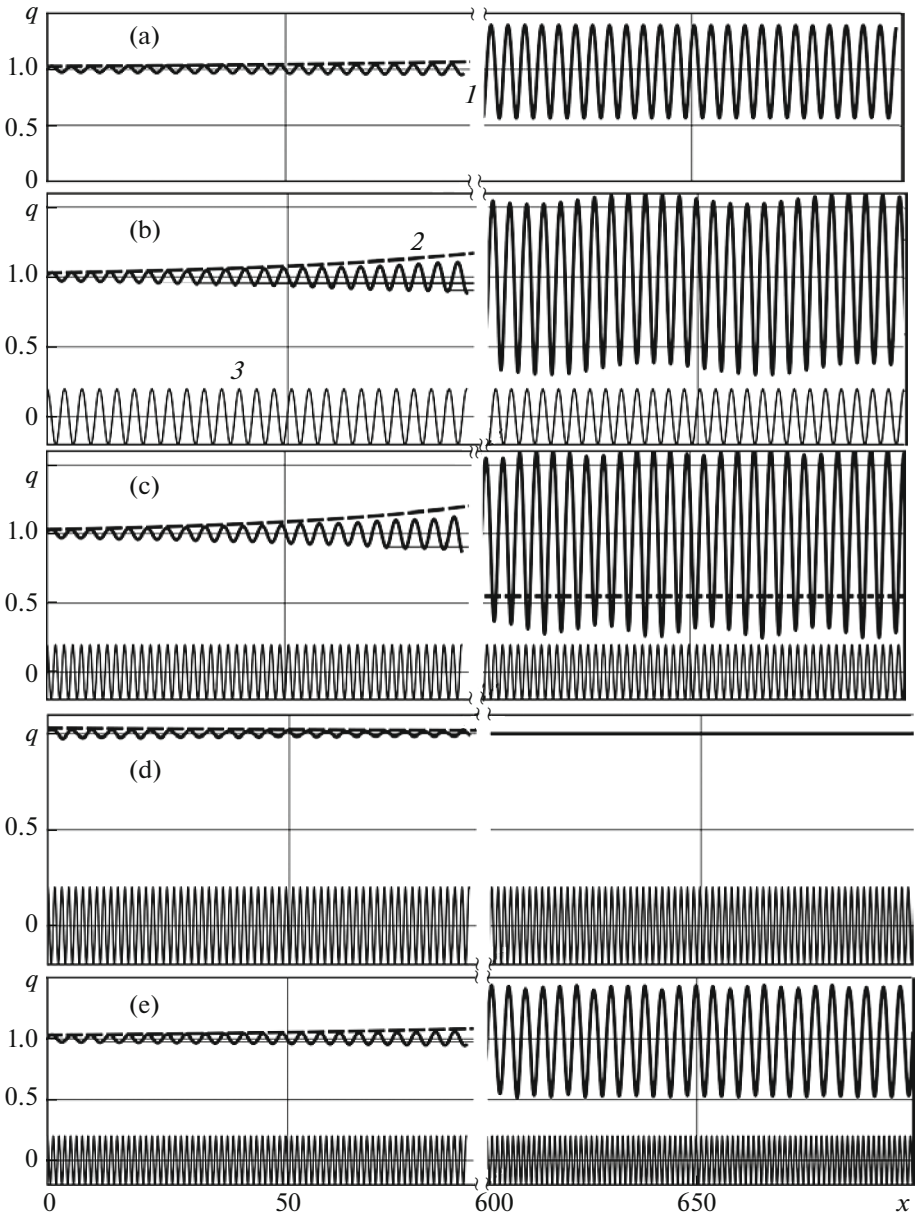

Fig. 5. Profiles of the high-frequency nonlinear waves: a corresponds to $a = 0$ and b–e to $s = 1$, 2, 2.5, and 3, respectively; curve *1* correspond to the free surface, curves *2* to the result of the linear stability theory, and curves *3* to the rigid surface.

where c is a certain constant. As shown in the previous section, the solution of the linearized problem is only slightly sensitive to variation in c, if $c > 2$ and L is fairly large.

Let a uniform grid with a step Δx be specified on a spatial segment and the finite-difference approximations

$$f_{xxx}(n\Delta x) = \frac{f_{n+2} - 3f_{n+1} + 3f_n - f_{n-1}}{\Delta x^3} + O(\Delta x),$$

$$f_x(n\Delta x) = \frac{f_n - f_{n-1}}{\Delta x} + O(\Delta x), \quad f_n = f(n\Delta x)$$

be used for the derivatives entering into (1.1).

The first-order scheme was taken since the use of central differences leads to the development of fast-growing shortwave numerical perturbations. The derivatives with respect to time were approximated

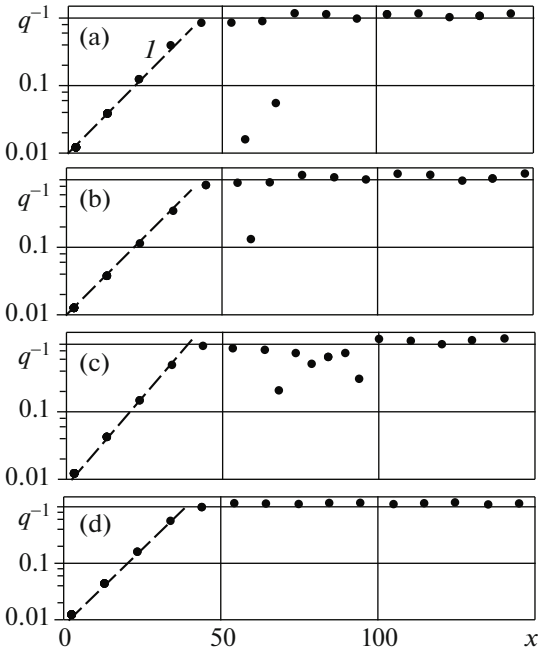

Fig. 6. Local maxima of the low-frequency nonlinear waves: a corresponds to $a = 0$ and b–d to $s = 1$, 2, and 3, respectively; lines *1* correspond to the result of the linear stability theory.

using the purely implicit scheme for stability reasons. The time step Δt was taken constant. The iteration method was used to solve the nonlinear algebraic equations, namely, for determining the next approximation the coefficients of the linear differential operators were calculated from the previous approximation.

The implicit-in-time scheme and the space approximation mentioned above introduce a small damping to the system; however, in the case of the scheme parameters $(\Delta t, \Delta x) \sim 10^{-3}$ the growth rates of small disturbances and the spatial period of the waves developed on the flat wall correspond to the linear theory (2.4) with the absolute error not greater than $3 \cdot 10^{-3}$.

The calculations were carried out with the initial conditions $q(0, x) = 1$ and $h(0, x) = h_s(x)$ and the boundary conditions $q(t, 0) = 1 + b \cos \omega t$ and $h(t, 0) = h_s(0)$ for $L = 290$, $\omega = 1.5$ and 4.5, and $a = 0.2$ for $s = 0.5, 1, 1.5, 2, 2.5$, and 3, as well was for $a = 0$. At small t a wave packet is formed. It contains waves of various frequencies due to the fact that transition from the boundary conditions $q = 1$ and $h = h_s$ to the nontrivial boundary conditions at $t \geq 0$ is equivalent to addition of perturbations at various frequencies. The periodic solution is formed after passage of the starting wave packet.

In Figs. 4 and 5 we have plotted the graphs of the functions $q(x)$ at fairly large $t = 3000\pi/\omega$ for various relief wavenumbers.

When $\omega = 1.5$ the disturbance growth rate varies only slightly due to the relief effect. The nonlinear waves represent the superposition of the solution corresponding to the flat wall and small waves close to harmonic waves with the wavenumber equal to the relief wavenumber α.

In accordance with the results of the linear stability analysis, the perturbations at the frequency $\omega = 4.5$ are stable for $s = 2.5$. In this case, perturbation damping is also observed in calculating the solution of the nonlinear equations. For other values of s the perturbations grow, the growth rate being close to that obtained in the linear theory at low amplitudes. The difference between the growth rates is of the order of 10^{-3} and can be attributable to the scheme viscosity. As the perturbations grow, the growth rate decreases and the saturation occurs. In flow down the flat wall the frequencies $\omega = 4.5$ form waves with the normalized wavenumber $s_0 \approx 0.91$. Longwave structures are formed in flow down the wall with the relief with $s = 1, 2$, and 3. In these structures the wave amplitude varies periodically only slightly.

In Figs. 6 and 7 we have reproduced the wave amplitude in the logarithmic scale, namely, the quantity $\ln(q - 1)$ has been plotted, the dotes correspond to the local maxima located above the mean level. The

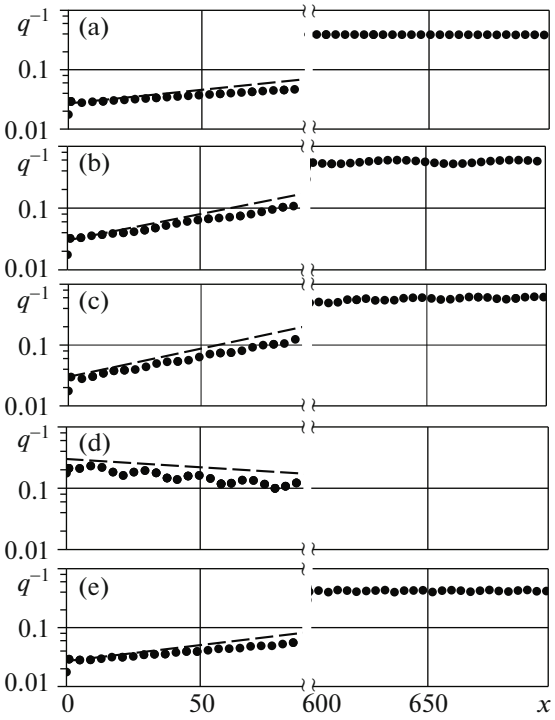

Fig. 7. Local maxima of the high-frequency nonlinear waves: a corresponds to $a = 0$ and b–e to $s = 1$, 2, 2.5, and 3, respectively; lines *1* correspond to the result of the linear stability theory.

broken curves show the result of the linear stability analysis and the mean amplitude of the steady-state waves. For the latter the spatial wave period is equal to the period of small perturbations at the same frequency. In accordance with the linear theory, for the amplitudes considered the relative change in this quantity is small with variation in the corrugation parameters.

The results obtained are in qualitative agreement with the experimental data [14] and the calculations of the full Navier–Stokes equations [13]. In the wave spectrum we can distinguish a wavenumber which corresponds to the frequency of variation in the boundary conditions for the flat wall, a wavenumber of the surface relief, and multiple wavenumbers, as well as the sums and differences of these wavenumbers, the basic harmonics predominating.

SUMMARY

The sinusoidal relief deposited on the vertical wall down which the viscous liquid film flows changes the wave parameters on the free surface. Using the Floquet theory, it is shown that the phase velocities and the growth rates are changed by a value proportional to the second power of the relief amplitude. For the corrections an approximate analytical solution which coincides well with the numerical calculations is obtained.

The resonance between the flow disturbances and the periodic relief whose wavenumber is greater than the wavenumber of neutral disturbances on the flat wall is revealed. Under the resonance the growth rate decreases appreciably and weakly growing disturbances are stabilized and become damped.

Nonlinear waves are simulated. The appearing wave structures replicate locally the steady-state waves on the flat wall; however, their amplitude varies slowly in the periodic manner.

The results obtained, in particular, the analytical expressions for the growth rates open the possibilities for the further qualitative analysis of the system considered: using the similar method, flow down the inclined plane with a microrelief can be studied and the detailed comparison with the results of the calculations [13] and the experiments [11, 14] can be carried out.

The work was studied with financial support from the Russian Foundation for Basic Research (project No. 15-01-05186) and the Council for Grants of the Russian Federation President (grant No. MK-1798.2017.1).

REFERENCES

1. S. J. Weinstein and K. J. Ruschak, "Coating Flows," Ann. Rev. Fluid Mech. **36** (1), 29–53 (2004).
2. E. I. Mogilevskii and V. Ya. Shkadov, "Effect of the Substrate Relief on the Non-Newtonian Liquid Film Flow down the Inclined Plane," Vestn. MGU, Matematika, Mekhanika 3, 49–56 (2007).
3. V. Ya. Shkadov, "Wave Flow Regimes of a Thin Layer of Viscous Fluid Subject to Gravity," Fluid Dynamics **2** (1), 29–34 (1967).
4. C. Heining, V. Bontozoglou, N. Aksel, and A. Wierschem, "Nonlinear Resonance in Viscous Films on Inclined Wavy Planes," Int. J. of Multiphase Flow **35**, 78–90 (2009).
5. D. Tseluiko, M. Blyth, and D. Papageorgiou, "Stability of Film Flow over Inclined Topography Based on a Long-Wave Nonlinear Model," J. of Fluid Mechanics **729**, 638–671 (2013).
6. C. Heining and N. Aksel, "Effects of Inertia and Surface Tension on a Power-Law Fluid Flowing Down a Wavy Incline," Int. J. of Multiphase Flow **36**, 847–857 (2010).
7. Yu. Ya. Trifonov, "Stability and Nonlinear Wave Regimes in a Film Flowing down a Corrugated Surface," Zh. Prikl. Mekh. Tekh. Fiz. **48** (1), 110–120 (2007).
8. K. Argyriadi, M. Vlachogiannis, and V. Bontozoglou, "Experimental Study of Inclined Film Flow along Periodic Corrugations: The Effect of Wall Steepness," Phys. Fluids **18**, 012102 (2006).
9. T. Pollak and N. Aksel, "Crucial Flow Stabilization and Multiple Instability Branches of Gravity-Driven Films over Topography," Phys. Fluids **25**, 024103 (2013).
10. Yu. Trifonov, "Stability of a Film Flowing down an Inclined Corrugated Plate: The Direct Navier–Stokes Computations and Floquet Theory," Phys. Fluids **26**, 114101 (2014).
11. M. Schoerner, D. Reck, and N. Aksel, "Stability Phenomena far beyond the Nusselt Flow Revealed by Experimental Asymptotics," Phys. Fluids. **28**, 022102 (2016).
12. E. A. Demekhin, G. Y. Tokarev, and V. Y. Shkadov, Hierarchy of Bifurcations of Space-Periodic Structures in a Nonlinear Model of Active Dissipative Media," Physica D **5** (2), 338–361 (1991).
13. Yu. Trifonov, "Nonlinear Waves on a Liquid Film Falling down an Inclined Corrugated Surface," Physics of Fluids **29**, 054104 (2017).
14. D. Reck and N. Aksel, "Experimental Study on the Evolution of Traveling Waves over an Undulated Incline," Physics of Fluids **25**, 102101 (2013).
15. V. Ya. Shkadov, "Wave-Flow Theory for a Thin Viscous Liquid Layer," Fluid Dynamics **3** (2), 12–15 (1967).
16. V. Ya. Shkadov, "Two-Parameter Model of Wave Regimes of Viscous Liquid Film Flow," Vestn. MGU, Matematika, Mekhanika **4**, 56–61 (2013).
17. C. S. Yih, "Stability of Liquid Flow down an Inclined Plane," Phys. Fluids **6** (3), 321–334 (1963).
18. V. Ya. Shkadov and E. A. Demekhin, "Wave Motions of Liquid Films on a Vertical Surface (Theory for Interpretation of Experiments)," Uspekhi Mekhaniki **4** (2), 3–65 (2006).
19. V. Ya. Shkadov and A. N. Beloglazkin, "Integral Relations of the Boundary Layer Theory in the Theory of Wave Capillary Film Flows," Vestn. MGU, Matematika, Mekhanika 6, 38–50 (2017).
20. V. A. Yakubovich and V. M. Starzhinskii, *Linear Differential Equations with Periodic Coefficients and their Applications* (Nauka, Moscow, 1972) [in Russian].
21. S. Kalliadasis, C. Ruyer-Quil, B. Scheid, and M. G. Velarde, *Falling Liquid Films* (Springer, London, 2012).
22. H. C. Chang, E. A. Demekhin, and E. Kalaidin, "Simulation of Noise-Driven Wave Dynamics on a Falling Film," AICHE Journal **42** (6), 1553–1568 (1996).